

5-2018

# Understanding the Coating-Substrate Interface Changes and Degradation Caused by Environmental Acclimation with Water and Electrolytes

Russell Vick

Follow this and additional works at: [https://aquila.usm.edu/honors\\_theses](https://aquila.usm.edu/honors_theses)



Part of the [Materials Chemistry Commons](#)

---

## Recommended Citation

Vick, Russell, "Understanding the Coating-Substrate Interface Changes and Degradation Caused by Environmental Acclimation with Water and Electrolytes" (2018). *Honors Theses*. 563.  
[https://aquila.usm.edu/honors\\_theses/563](https://aquila.usm.edu/honors_theses/563)

This Honors College Thesis is brought to you for free and open access by the Honors College at The Aquila Digital Community. It has been accepted for inclusion in Honors Theses by an authorized administrator of The Aquila Digital Community. For more information, please contact [Joshua.Cromwell@usm.edu](mailto:Joshua.Cromwell@usm.edu).

The University of Southern Mississippi

Understanding the Coating-Substrate Interface Changes and Degradation Caused by  
Environmental Acclimation with Water and Electrolytes

by

Russell Vick

A Thesis  
Submitted to the Honors College of  
The University of Southern Mississippi  
in Partial Fulfillment  
of the Requirements for the Degree of  
Bachelor of Science  
in the Department of Polymer Science and Engineering

May 2018



Approved by

---

James Rawlins, Ph.D., Thesis Advisor  
School of Polymer Science and Engineering

---

Jeffrey Wiggins, Ph.D., Director  
School of Polymer Science and Engineering

---

Ellen Weinauer, Ph.D., Dean  
Honors College

## Abstract

While it is well known that polymeric coatings are used to protect metals from corrosion, efficient and reliable protocols for quantifying and estimating protective coatings' lifetimes have yet to match real-time results in rate or in detected mechanisms of material failure. Alkoxysilane pretreatments are widely utilized for substrate preparation and improved coating system performance by changing the metal substrate surface morphology to improve adhesion at the coating-substrate interface by creating a foundation and excluding water from the system. Three pretreatments used were 3-aminopropyltriethoxy silane (APS), tetraethylortho silicate (TEOS), N-[3-(trimethoxysilyl)propyl]ethylenediamine (DAS). They were investigated to improve the understanding of the relationships between the silane solution and the physical and chemical structure of the resulting pretreatment layer. They were also investigated to correlate the pretreatment structure with the charge transfer resistance at the interface to quantify and understand the contribution charge transfer resistance has on the silane pretreatment's anti-corrosive performance. It was determined using Infrared Spectroscopy that the most uniform silane network was generated when the silane to water molar ratio was low. The pretreatment results were validated with pull-off adhesion results using Mechanical Testing System (MTS). Further, the charge transfer resistance and instantaneous rate of corrosion of silane pretreated substrates is heavily dependent on the thickness and structure of the silane, as shown using Electrochemical Impedance Spectroscopy (EIS) and Electrochemical Frequency Modulation (EFM).

Keywords: Alkoxysilane, 3-aminopropyltriethoxy silane, tetraethylortho silicate, N-[3-(trimethoxysilyl)propyl]ethylenediamine, interface, charge transfer resistance

## **Dedication**

To my parents, Marty and Cindy, for always pushing me to do my very best in all my years of education.

## **Acknowledgements**

I would like to thank my advisor, Dr. James Rawlins, for his consultations and support throughout this project and my educational career here at The University of Southern Mississippi. Not once was he ever too busy to make time for me, attend to my scientific curiosity, and challenge me intellectually.

I would also like to thank Diana Gottschalk and the rest of the Thames-Rawlins Research Group for their guidance, patience, and input throughout my research and time in the lab. Never did I find myself unable to sit down with a colleague and try to solve any issues I came across. Thank you all for your support and friendship.

## Table of Contents

List of Tables .....	viii
List of Figures .....	ix
List of Abbreviations .....	x
Chapter I. Introduction.....	1
Chapter II. Literature Review .....	3
Corrosion and Organic Coatings .....	3
Silane Pretreatments .....	6
Experimental Rationale .....	7
Chapter III. Methodology .....	10
Materials.....	10
Sample Preparation and Characterization .....	11
APS solutions and Near-IR Spectroscopy .....	11
Preparation and Analysis of APS for Attenuated Total Reflectance-IR Spectroscopy .....	11
Preparation and Deposition of Alkoxysilane to Substrate.....	12
Pull-off Adhesion of DAS Samples.....	12
Characterization of Silane Pretreatment Thickness.....	14
EIS and EFM of TEOS films.....	14
Chapter IV. Results and Discussion.....	15
Near-IR and ATR-FTIR Analysis .....	15
Pull-off Adhesion of DAS Samples .....	20
Resistance and Corrosion Related to Physical Properties of Silane Film.....	21
Chapter V. Conclusions and Future Works .....	26
References.....	28



## List of Tables

Table 1: APS Sample Composition.....	11
Table 2: DAS and G9V10BII Compositions.....	12
Table 3: Composition of TEOS Samples.....	14
Table 4: Differential Mass and Theoretical Thickness Results.....	21
Table 5: EIS and EFM Results.....	23

## List of Figures

Figure 1: Ion transport diagram.....	5
Figure 2: Delamination, blistering, and dissolution of a coated substrate.....	6
Figure 3: Electron flow chart during cathodic delamination.....	7
Figure 4: Silane reaction scheme.....	8
Figure 5: Structure of silane pretreatment at various concentrations.....	9
Figure 6. MTS Pull-off Adhesion Load Frame.....	13
Figure 7: Near-IR Spectroscopy of T0 APS Solution Samples.....	16
Figure 8: Near-IR Spectroscopy of Teq APS Solution Samples.....	16
Figure 9: Silanol and Water Concentrations in Teq Solutions.....	17
Figure 10: ATR-FTIR of APS Solutions Compared to APS Standard.....	18
Figure 11: ATR-FTIR of Solid APS Networks.....	19
Figure 12: Siloxane and Silanol Peak Areas.....	19
Figure 13: Pull-off Adhesion Data of DAS Samples and Control.....	21
Figure 14: Open Circuit Potential of EIS/EFM Samples.....	22
Figure 15: Nyquist plot of TEOS Samples .....	23
Figure 16: Charge Transfer Resistance vs. Silane Thickness.....	24
Figure 17: Instantaneous Rate of Corrosion vs. Silane Thickness.....	25

## **List of Abbreviations**

ATR-FTIR – Attenuated Total Reflectance – Fourier Transform Infrared Spectroscopy

Near-IR – Near – Infrared Spectroscopy

EIS – Electrochemical Impedance Spectroscopy

EFM – Electrochemical Frequency Modulation

APS - 3-Aminopropyltriethoxy silane

DAS - N-[3-(Trimethoxysilyl)propyl]ethylenediamine

TEOS - Tetraethylortho silicate

MTS – Mechanical Testing System

## **Chapter I. Introduction**

Along with the monetary burden associated with eventual corrosion of metal assets, coating formulations have an additional sizeable time and effort cost for validation, testing, utilization and eventual replacement. Before coatings are commercialized, months and even years are dedicated to rigorous testing to predict the corrosion and adhesion performance after application in the field. A standard accelerated weathering test consists of 10,000 hours (416 days) under salt spray to simulate a few of the mechanistic aspects occurring in a marine/coastal environment. However, if the relationships between coating structures and their protective mechanisms are quantified and more fully understood, then the efficiency of utilization and approval is improved dramatically; years of testing and the overall cost of new material solutions can be reduced. If surface coating scientists can detect and quantify precursor events that correlate with long term performance, then we could calculate and predict a formulation's performance based on sound scientific relationships. The results could increase the rate of material development and make better use of the time and money spent on that development. The ideal scenario would be to run brief, but relevant, characterization on a coating substrate combination from which failure rates can be predicted. Chemists could pinpoint an accurate time of material changes, such as delamination, rather than spending thousands of hours to answer the question: "When will this coating fail?".

The most common way to protect metal assets from environmentally driven corrosion is to coat them with polymeric coatings. While a sizeable amount of coatings is used for aesthetic purposes, protective coatings are made specifically for corrosion protection. When a coating is applied to a substrate, an interface forms. The two-

dimensional surface where the two materials physically meet is where most of the corrosion reactions happen. After water, electrolytes, and oxygen permeate the coating, they begin to accumulate at the coating-substrate interface, and the metal substrate becomes electrically active. The corrosion processes include metal dissolution, ion transport, charge transfer, and oxidation of water. Production of metal hydroxides (e.g.  $\text{Fe}(\text{OH})_2$ ) depends on the transfer of a free electron in the metal with water molecules across the interface. One mechanism of corrosion protection of a coating system is to increase the energy required for electrical charge transfer to occur, thus lowering the corrosion rate.

Surface pretreatments are often applied prior to the coating and provide dramatically differing degrees of wetting and adhesion from the same coating system thus resulting in different anti-corrosive properties. A common pretreatment chemistry is the silane pretreatment; the materials are designed to provide a thin, and yet dense, crosslinked layer that minimizes the adhesion loss due to the degradative hydroxide across the interface by reducing accumulation of environmental contamination at that interface and increasing bond strength. Silane pretreatments were chosen for this project over other pretreatments as they have been shown to be more industrially and environmentally friendly.

The objectives of this project were to 1) understand the relationships between silane solution formulation and the physical and chemical structure of the resulting pretreatment layer and 2) to correlate pretreatment structure with charge transfer resistance. Completion of these objectives allows coatings chemists to be steps closer to testing their coatings much more efficiently. The systems investigated consisted of steel

substrates, as steel is a common metal used worldwide, treated individually with 3-aminopropyltriethoxy silane (APS), N-[3-(trimethoxysilyl)propyl]ethylenediamine (DAS), and tetraethylortho silicate (TEOS). The relationships between silane solution compositions and the physical and chemical structure of the resulting pretreatment film were investigated and validated. Charge transfer resistance and instantaneous corrosion rates of silane films were correlated to theoretical network thicknesses. Employment of these strategies were the first of many steps taken to eventually lead to the understanding of any contributing interfacial factors of coating-substrate degradation and the quantification of its relationship with charge transfer.

## **Chapter II. Literature Review**

### **Corrosion and Organic Coatings**

Corrosion is the thermodynamically favorable reaction of oxygen and water with an elemental metal. If metal is left unprotected, it will corrode once it encounters water, salts, and oxygen. Without electrolytes being present, water would have little to no conductivity.<sup>1</sup> Conductivity in water promotes charge transfer by making the water molecules more active and subject to oxidation reduction reactions. The reactions produce an oxidized and more chemically stable, but mechanically weaker, form of the metal. When metals are corroded, their physical integrity becomes severely compromised and the material can no longer perform the required structural function and can become a safety hazard. Unfortunately, some of the more electrochemically active metals have the more desirable structural properties. Steel is an excellent example of a metal alloy that is very strong and widely used but also prone to corrosion. Both anodic

and cathodic areas are present on steel surfaces due to the alloy containing different electric potentials. At the anodic site in the presence of water, electrolytes, and oxygen, iron will oxidize and solubilize while also releasing electrons. The charge transfer events that occur are essential to the corrosion reactions. Charge transfer allows generated electrons to fuel the cathodic site to reduce water and oxygen into hydroxides which further promote the dissolution and overall corrosion of the metal.<sup>1</sup>

A cost-effective way to combat corrosion is by applying a protective organic coating to the metal to keep the harmful marine environment away from the surface.<sup>1</sup> Surface coating scientists and engineers have a wide range of different polymer coating systems that can be tailored to fighting corrosion or improving other properties. Polyurethane and polyester coatings are common chemistries for corrosion control coatings. Due to their electric insulating properties polymeric organic coatings act as a barrier to charge transfer from the anode to the cathode at the interface.<sup>1</sup> While coatings do interfere with charge transfer, the materials are not isotropic, are not perfect physical, chemical or electrical barriers, and do not last forever. Water, electrolytes, and oxygen will still reach the coating-substrate interface, destroy the coating-substrate interface, and cause corrosion over time.

Ion transport is an event where electrolytes create pathways for water and oxygen to travel to the coating-substrate interface. Even with a protective polymer coating, corrosion can still occur and spread throughout the substrate due to ion transport, water and oxygen infiltration, and ultimately accumulation at the metal interface. Physical defect, bulk transport through the coating, and interfacial transport are the main modes of ion transportation and are shown in Figure 1. Wicks discusses that physical defect to the

coating post-application could allow for corrosion to occur because the substrate could be exposed to the environment.<sup>2</sup> Leng conveys that small molecules like sodium and chlorine, as solvent separated or individual ions, can migrate through thin polymeric films simply by wedging between the coating molecules and making paths for water and oxygen.<sup>3</sup> Once water, oxygen, and electrolytes reach the coating-substrate interface, regardless of the mode of transport, those corrosive reagents can spread easily throughout the interface, thus allowing charge transfer to occur.<sup>4</sup> When this happens, the metal surface becomes cathodically polarized, allowing the production of metal hydroxides to form at the substrate's surface in the presence of electrolytes. The hydroxide ions are very dangerous because they cause coating-substrate interface degradation to occur. Figure 2 illustrates the blistering, dissolution, and delamination that can occur when water, oxygen, and electrolytes reach the interface.<sup>5</sup>

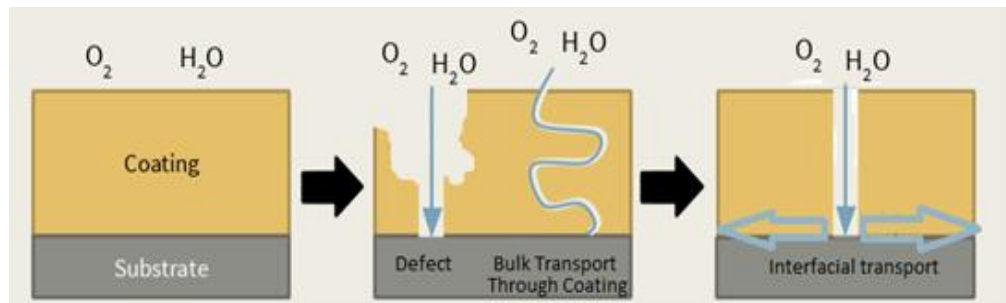


**Figure 1:** Ion transport diagram.



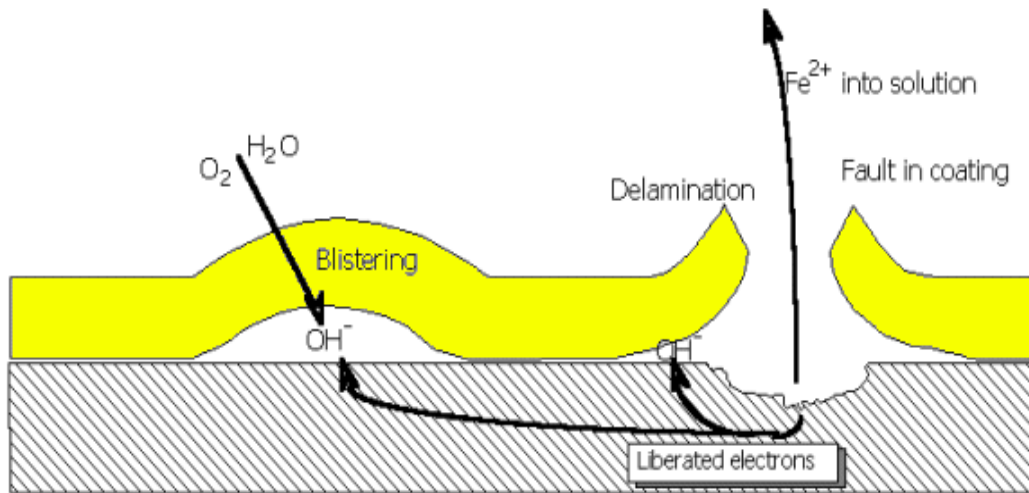


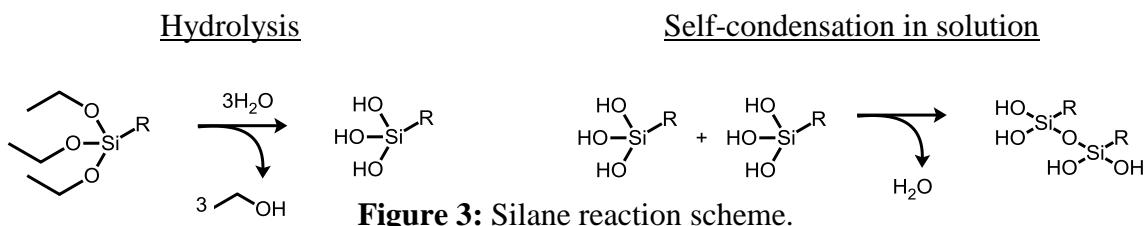
**Figure 2:** Delamination, blistering, and dissolution of a coated substrate.

### Silane Pretreatments

One of the biggest steps the coatings industry needs to take is to develop coatings that do not allow electrons to travel across the interface. By reducing the amount of void space at the interface, the migration tendency of water, oxygen, and electrolytes is minimized.<sup>4</sup> Prior to coating application a pretreatment can be used to treat the substrate, improving interfacial properties. Chromate pretreatments have been widely used as pretreatments for metal surfaces. Because working with heavy metals is toxic to people and the environment, other pretreatments have been sought out and developed.<sup>6</sup>

Silane pretreatments are effective in improving interfacial properties due to their ability to self-assemble along the surface and bond to both the substrate and the coating.<sup>7</sup> Silane pretreatment reactions involve the initial hydrolysis of alkoxy silane molecules with water to form silanol groups. After a specified hydrolysis time, metals are typically

treated at this point in the reaction. These silanols then can self-condense with other silanols to form a network of conjoined silane molecules. Also, the silanols can condense with metal hydroxides on the surface. This allows a network to be formed that is directly bonded to the substrate. Side groups on silane molecules, such as APS's amine side group, can also react with and bond to certain coatings. This demonstrates how silanes can be bonded to both the coating and substrate. The hydrolysis and self-condensation reactions are shown in Figure 3 below.



### Experimental Rationale

The ideal case for silane pretreatment application is the formation of a well connected monolayer covalently bound to both the substrate and coating. Applying a monolayer is possible by promoting hydrolysis over condensation in solution and acceleration of condensation after application. If condensation in solution is favored over hydrolysis, then there is less control over the structure of the film and a greater chance of poor packing at the interface. Silane solution compositions can be altered to experience different rates and extents of hydrolysis to give a variety of different surface structures. Figure 4 illustrates generally how these different concentrations may vary structurally from each other. Just by changing the concentration of silane in solution alone, J. Bertho and his research group found varying adhesion in coated/pretreated metals.<sup>8</sup> It is clear that altering the silane in solution will give different structural properties.

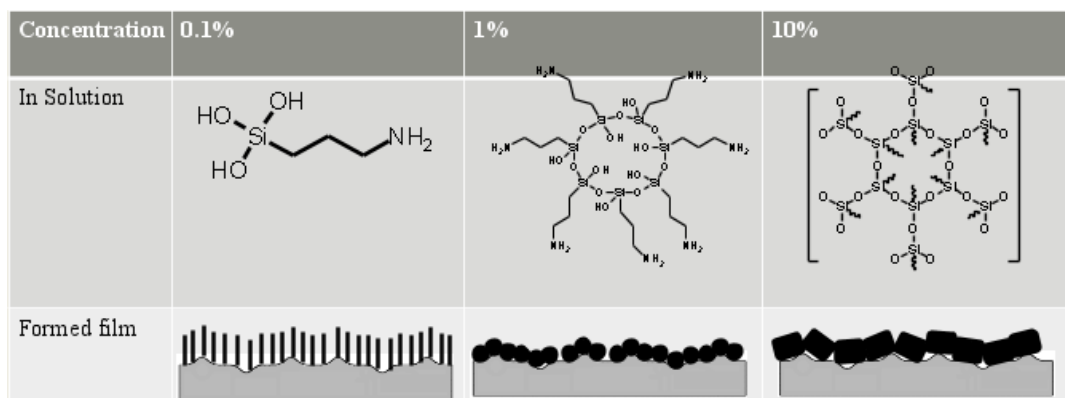


**Figure 4:** Structure of silane pretreatment at various concentrations.

The characterization of silanes in solution gives opportunity to further investigate silane solutions apart from just changing the concentration. Extent of hydrolysis and self-condensation of silanes in solution can be monitored via Infrared Spectroscopy.<sup>9,10</sup> By hydrolyzing silanes with different amounts of water rather than simply changing silane concentration, the structure of the solid network should be different and exhibit different properties in adhesion and water exclusion. By investigating the effect water content has on silane pretreatments, more efficiently packing silane networks can be discovered. Along with understanding how to manipulate the silane structure at the interface, understanding the properties that follow is also important.

While coatings act as a barrier to charge transfer at the coating-substrate interface, charge transfer still will occur over time as ions transport throughout the interface.<sup>1</sup> Figure 5 illustrates the ions present and charge transfer that occurs at the coating-substrate interface when water, oxygen, and electrolytes are present. Coatings provide resistance to charge transfer at the coating-substrate interface that can be measured. Electrochemical Impedance Spectroscopy can be used to measure the charge transfer resistance at the coating-substrate interface to determine adhesion loss and corrosion

caused by interfacial degradation.<sup>11,12</sup> Also, Electrochemical Modulation Frequency can be used to determine the instantaneous rates of corrosion at the coating-substrate interface.<sup>13</sup>

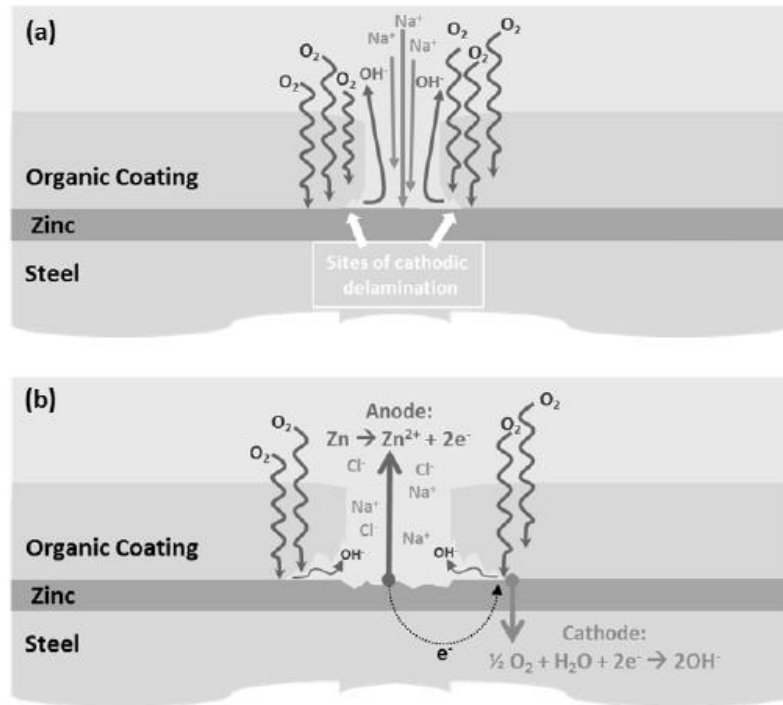


**Figure 5:** Ions and charge transfer present on coated substrates.

By performing EIS and EFM on silane pretreated substrates, information about the charge transfer resistance and instantaneous rates of corrosion can be gained. With concentration of silane solution being the variable, the corresponding thickness of the silane layer should change. The changes in thickness should affect the amount of charge transfer resistance and the instantaneous rate of corrosion. Thus, the dependence that resistance and instantaneous rate of corrosion have on the silane pretreatment thickness can be further understood.

Understanding how the silane network is formed as well as the electrochemical properties that result from those networks is very important to achieving the goal of predicting coating failure due to corrosion. Current methods using a salt fog as accelerated testing simply take too much time. Given the amount of literature present using IR spectroscopy along with EIS and EFM to characterize silanes and the coating substrate interface, understanding of silane pretreatment networks and their properties using these characterization methods appeared to be achievable.

### **Chapter III. Methodology**

#### **Materials**

Pretreatment solutions were composed of alcohol (reagent ethanol or methanol supplied by Fisher Scientific), deionized water produced from an in-house filtration system and an alkoxy silane. One of three alkoxy silanes were included to study specifically adhesion and electrochemical properties; 3-aminopropyltriethoxy silane (APS, 98% from Gelest, Inc.), N-[3-(trimethoxysilyl)propyl]ethylenediamine (DAS, 97% from Acros) and tetraethylortho silicate (TEOS, 98% from Sigma Aldrich) were each used as received.

Epoxy amine coatings were formulated with Epon 825 used as received from Hexion, Inc, benzyl amine (99% purchased from Acros), Jeffamine ED-600 (95% from Huntsman) and 1,3 bisaminomethyl cyclohexane (BAC, 98%) were purchased from TCI Chemicals. After initial bodying of the monomer, mixture solvent was added to improve film formation, specifically toluene (99%) and di(propylene glycol) propylether (DPnP, 98%) purchased from Sigma Aldrich. Glacial acetic acid (HAc, 99%) was purchased

from Fisher Scientific. Low carbon, cold rolled steel panels with low roughness (QD-36) were purchased from Q Labs. All chemicals were used as received.

## Sample Preparation and Characterization

### *APS solutions and Near-IR Spectroscopy*

**Table 1:** APS Sample Compositions.

Sample	APS	H <sub>2</sub> O	Ethanol
30% APS 1:1	1.5g	0.12g	3.4g
30% APS 1:2	1.5g	0.24g	3.3g
30% APS 1:3	1.5g	0.37g	3.1g

Three different 30 wt% APS solutions with 1:1, 1:2, and 1:3 molar ratios of silane to water were generated according to Table 1. The solutions were mechanically stirred for 24 hours to allow hydrolysis to reach equilibrium. Aliquots of 170 microliters were taken from the sample solutions to quantify chemical composition with Near-IR spectroscopy immediately after homogenization and after 24 hours. Spectra were collected on an integrating sphere in transmission mode by placing a reflective surface over the vial. 32 scans were taken at a resolution of 2 cm<sup>-1</sup>.

### *Preparation and Analysis of APS for Attenuated Total Reflectance-IR Spectroscopy*

To complement the alkane and water information obtained from the Near-IR spectra with silicon species, a few drops of the previously equilibrated APS solution samples were placed onto the ATR-FTIR for analysis at a resolution of 4 cm<sup>-1</sup> for 128 scans. A cover was placed on top of the detector to minimize solvent evaporation and

composition changes during the measurement. Solution spectra were compared with spectra of condensed silane networks prepared by isolating two milliliters of each of the three APS samples inside separate scintillation vials, which were then placed into a vacuum oven at 80 °C overnight. The solid samples were then analyzed by ATR-FTIR spectroscopy following the same parameters as the solutions.

*Preparation and Deposition of Alkoxysilane to Substrate*

Each silane pretreatment deposition was performed using the same method. First, the silane solutions were allowed to hydrolyze. Then steel panels were cleaned with mineral spirits, dried, and submerged into the hydrolyzed silane solution for 30 seconds. After immersion, the panels were rinsed with deionized water, and dried using flowing nitrogen gas. Finally, the treated panels were cured in the oven at 100 °C for one hour.

*Pull-off Adhesion of DAS Samples*

**Table 2:** DAS and G9V10BII Compositions.

Sample	DAS		H <sub>2</sub> O	Methanol		
30% DAS 1:1	9g		0.73g	20.3g		
30% DAS 1:2	9g		1.46g	19.5g		
30% DAS 1:3	9g		2.19g	18.8g		
Epoxy Amine Coating	Epon 825	Benzyl Amine	1-3 BAC	Jeffamine ED-600	Toluene	DPnP
	10.02g	0.708g	0.791g	3.49g	1.88g	1.88g

DAS samples of 1:1, 1:2, and 1:3 silane to water molar ratios were mixed, deposited, and cured onto cleaned panels using the method described above. Treated

panels were then coated via draw down with a model epoxy amine formulation (G9V10BII) at four wet mils. The panels were left at ambient temperature for 24 hours in a dry box followed by a final cure for four hours in an oven at 80 °C. The composition of the DAS solutions and G9V10BII coating are shown in Table 2. Next, aluminum studs were glued onto the coating surface using a two-part epoxy amine glue, Scotch-Weld DP 460. Once the glue was cured, the studs were pulled off using a Mechanical Testing System load frame as depicted in Figure 6. The studs were pulled off at two mm/min and the stress required to separate the stud from the panel was recorded.



**Figure 6:** MTS Pull-Off Adhesion Load Frame.



### *Characterization of Silane Pretreatment Thickness*

**Table 3:** Composition of TEOS samples.

Sample	TEOS	Ethanol	Acetic Acid	H <sub>2</sub> O
10% TEOS	9g	18.72g	1.5g	0.778g
20% TEOS	6g	22.48g	1g	0.519g
30% TEOS	3g	26.24g	0.5g	0.259g

Aluminum disks with a 12.5 mm diameter were used to calculate the mass per unit area of varying concentrations of TEOS samples to estimate film thickness. The disks were weighed using a Sartorius analytical balance with accuracy to a thousandth of a milligram before being treated with a 10%, 20%, or 30% TEOS solution, each with a 1:1 molar ratio of silane:water (composition of the TEOS solutions are listed in Table 3). Disks were treated using the technique described previously except without rinsing. Rinsing was eliminated to ensure that a statistically significant mass change could be recorded. The unrinsed samples should still hold the same structural relationships of all three TEOS samples as if they were rinsed. The disks were cured at 100 °C for one hour and then reweighed. The mass change was recorded and the mass per unit area was calculated for each concentration, which finally led to a calculation of the theoretical thickness of each sample. This calculation was performed by dividing the gained mass by the product of the surface area and density (1.65 g/cm<sup>3</sup>) of the TEOS.<sup>14</sup>

#### *EIS and EFM of TEOS films*

Steel panels were treated with either 10%, 20%, or 30% TEOS as described above. The TEOS panels were used as the working electrodes to perform Electrochemical

Impedance Spectroscopy and Electrochemical Frequency Modulation to find the charge transfer resistance and instantaneous rates of corrosion, respectively. A cleaned and untreated panel was also analyzed as a control. Of the 2 x 3 inch panel surface, the majority was sealed with tape and only a circle 2 mm in diameter was exposed to a salt solution. The panels were connected to a Gamry Potentiostat/Galvanostat while a 40 mm diameter cell filled with 30 ml 5% NaCl in solution was clamped onto the taped substrate. An open circuit potential was taken for 30 minutes on all of the panels before EIS or EFM were performed to make sure they were stabilized.

EIS was performed at a 5 mV AC voltage across a frequency range from 100 kHz and 0.01 Hz respectively. The points/decade was 7 and it took approximately 30 minutes to perform the EIS experiment per sample. EFM was performed at a base frequency of 0.1 Hz. The A and B multipliers were set at 2 and 5, respectively. The amplitude was 10 mV. Three EFM scans were taken per sample in quick succession to ensure the instantaneous rates of corrosion were consistent.

## **Chapter IV. Results and Discussion**

### **Near-IR and ATR-FTIR Analysis**

Near-IR spectroscopy allows for the quantification of water consumed during hydrolysis. Solution spectra of 30% APS at time zero and 24 hours are shown in Figures 7 and 8, respectively. Looking at the difference in the water band at  $5160\text{ cm}^{-1}$ , it can be concluded that water is consumed during hydrolysis. Figure 9 illustrates the absorbances of silanols and water that are present in each of the three samples after hydrolysis occurs. Considering that water is consumed during hydrolysis, the differential between the  $t_0$ 's

and  $t_{eq}$ 's water concentration should be equal to the amount of silanols formed.

Assuming complete hydrolysis, any remaining water can be designated as water evolved during self-condensation.

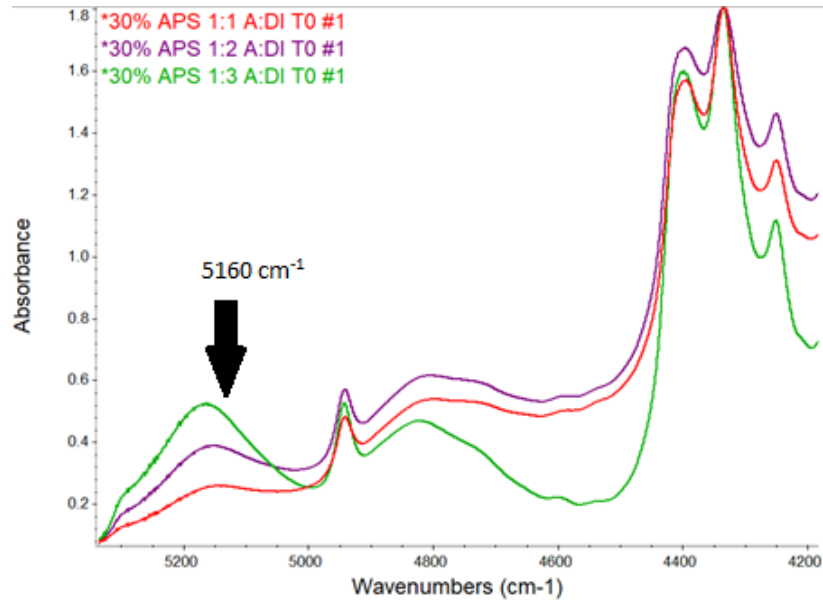


**Figure 7:** Near-IR Spectroscopy of  $t_0$  APS Solution Samples.

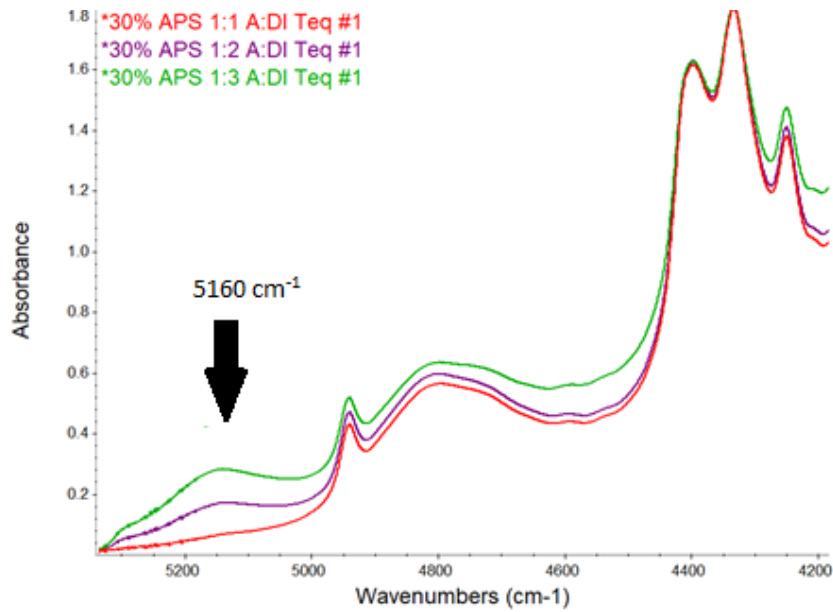


**Figure 8:** Near-IR Spectroscopy of  $t_{eq}$  APS Solution Samples.

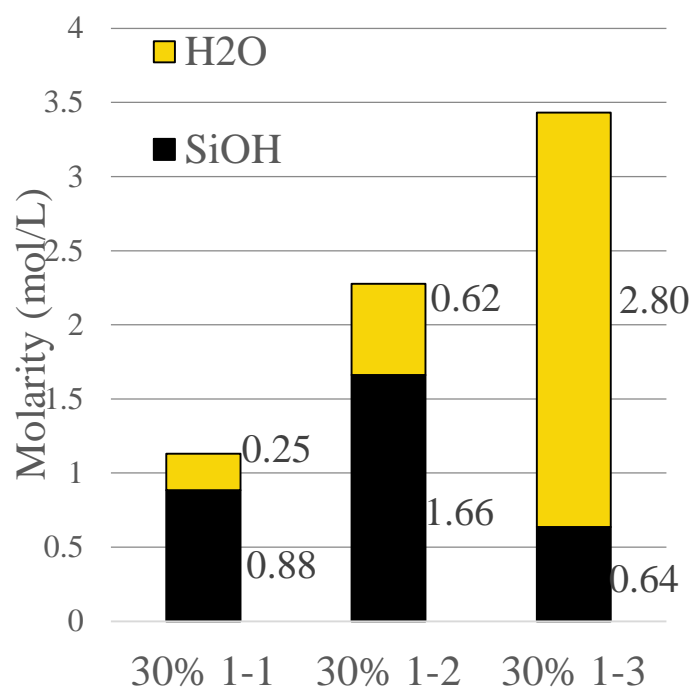


**Figure 9:** Silanol and Water Concentrations in  $t_{eq}$  Solutions.

By comparing the silane concentration to the equilibrium water concentration, a trend is visible in that increasing the silane water ratio increased the extent of self-condensation. It is reasonable to conclude that because the 1:3 sample had the highest water content, it achieved the highest extent of hydrolysis and inevitably self-condensed more than the other two samples in solution. The silanol concentration does not follow the same trend as the water condensation; the 1:1 and 1:2 samples showed increasing silanol concentrations due to the increasing amounts of water added, but 1:3 sample had the lowest silanol concentration. This could be due to the excessive self-condensation that occurred as shown by the higher water concentration. This means that overall the 1:3 sample resulted in such vast hydrolysis that the silanols were being consumed by condensation.

The ATR-FTIR spectroscopic analysis concluded that each of the 30% APS samples had negligible amounts of alkoxy groups remaining after 24 hours of mechanical stirring. This is shown in Figure 10 by the minimum absorbance present at the Si-O-Et peak present at  $951\text{ cm}^{-1}$  when compared to a standard. The spectra support that all of the achievable hydrolysis had occurred during processing.

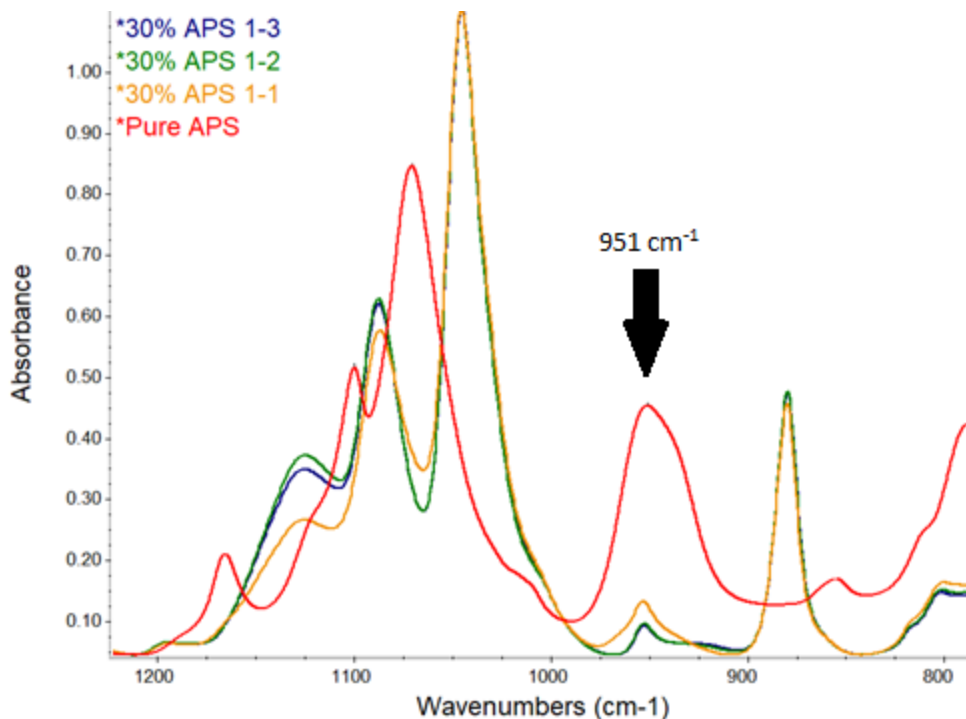


**Figure 10:** ATR-FTIR of APS Solutions Compared to APS Standard.

The ATR-FTIR analysis of the condensed APS samples, Figures 11 and 12, concluded that the highest degree of siloxane bond formation ( $1120\text{ cm}^{-1}$ ) occurred in the 1:1 ratio solid sample while the fewest were in the 1:3 network. The peak area is directly proportional, but not equal, to the concentration. Despite having the most self-condensation in solution, the 1:3 sample had the lowest Si-O-Si concentration in solid form. The silanol concentration trend stayed the same between solution and solid forms.

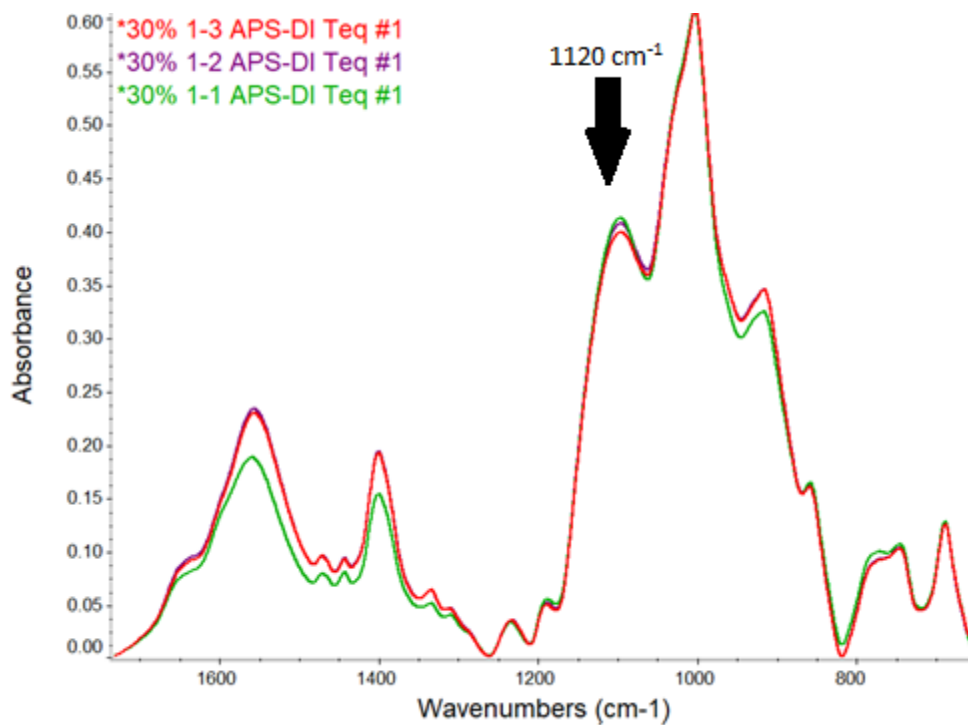


**Figure 11:** ATR-FTIR of Solid APS Networks.

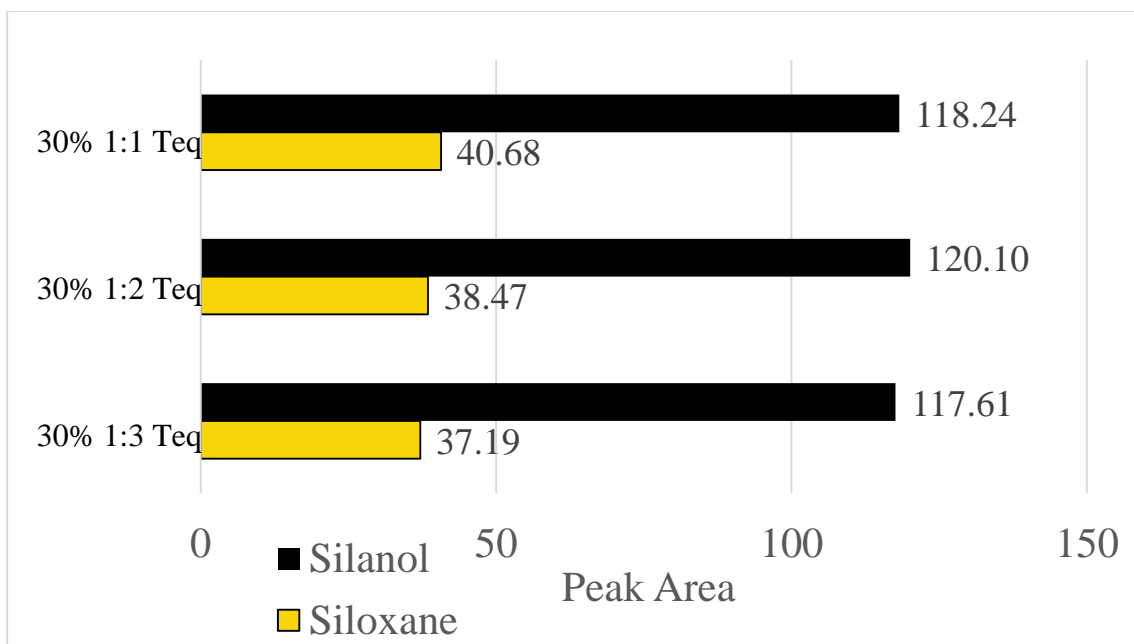


**Figure 12:** Siloxane and Silanol Peak Areas.

Producing a silane pretreatment with the highest density of siloxane bonds in the solid state requires minimum amounts of the self-condensation that occurs in solution. It is very likely that, because the 1:3 silane to water sample reacted and condensed so much in solution, it formed higher molecular weight or cyclic species. When the solidification process and curing occurred, the higher molecular weight and cyclic species were already formed, thus getting in the way of forming a tightly packed network. The 1:1 sample likely formed the most uniform film because it condensed the least in solution and had the highest amount of Si-O-Si bonds in the solid state. This difference in absorbance at the  $1120\text{ cm}^{-1}$  standard Si-O-Si peak, while it may seem minimal, likely illustrates differences in surface uniformity, which in turn affects coating performance properties such as pull-off adhesion.

### **Pull-off Adhesion of DAS Samples**

DAS was used to probe interfacial strength, as it has similar alkoxy silane reactivity as APS but with more amine functionality. The increase in amine functionality makes DAS a more viable adhesion promoter and should have made the differential in adhesion clearer. The pull-off adhesion testing of the DAS samples found that increasing the concentration of water decreased the peak stress required for pull-off (Figure 13). A more uniform silane film is going to have improved connectivity between the coating and the substrate, increasing the measured mechanical adhesion. Under the assumption that the DAS reactivity is similar to APS, this adhesion data validated that the most uniform siloxane film is gained by minimizing the amount of condensation that occurs in solution and maximizing the amount of Si-O-Si bonds in the solid phase. Interestingly, the 1:2 and 1:3 samples showed an average decrease in adhesion compared to the control

G9V10BII sample. It is probable that the surface morphology of the pretreated 1:2 and 1:3 panels were not uniform enough to improve the adhesion and actually decreased it.

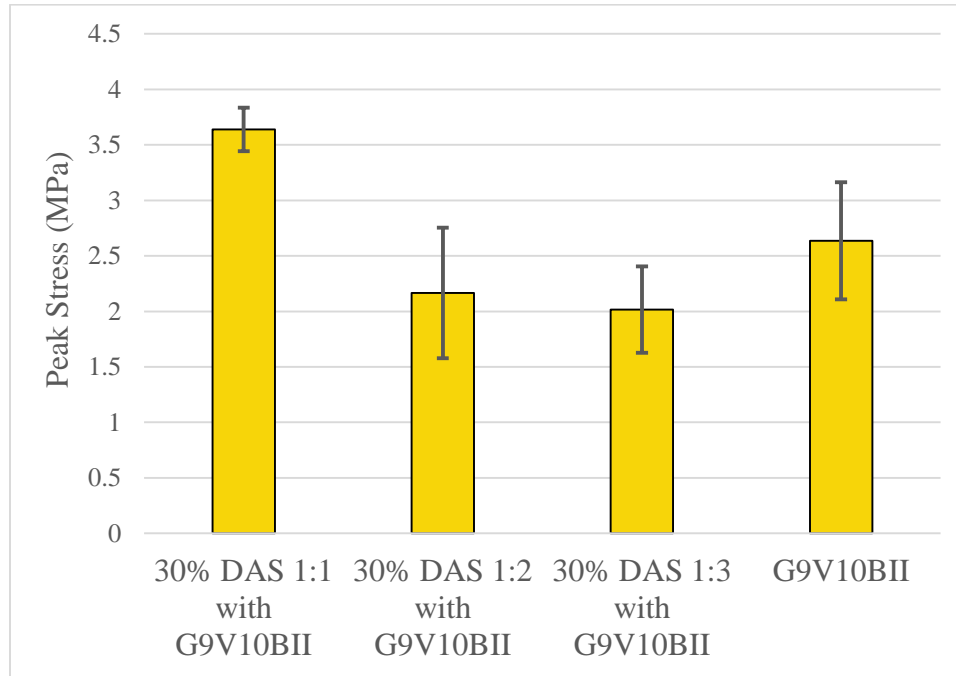


**Figure 13:** Pull-off Adhesion Data of DAS Samples and Control.

### Resistance and Corrosion Related to Physical Properties of Silane Film

**Table 4:** Differential Mass and Theoretical Thickness Results.

Sample	Average Mass Increase (mg)	Disc Surface Area (mm <sup>2</sup> )	Mass per Surface Area (g/cm <sup>2</sup> )	Theoretical Thickness (microns)
10% TEOS	0.0125	278.03	4.50x10 <sup>-6</sup>	0.027
20% TEOS	0.0655	278.03	2.36x10 <sup>-5</sup>	0.143
30% TEOS	0.110	278.03	3.96x10 <sup>-5</sup>	0.240

The masses of the 10%, 20%, and 30% treated disks before and after pretreatment, calculated mass per unit areas of the silane networks, and theoretical



thicknesses are reported in Table 4. The mass per unit area increased with the percent TEOS in the pretreating solution, confirming that more silane in solution increases the silane that is deposited on the substrate. These calculated values were used to normalize the charge transfer resistance and rate of corrosion.

The open circuit potentials of the TEOS samples are shown in Figure 14. The plateau present in each of the curves signifies that the samples were stabilized before EIS and EFM were performed. The EIS data for TEOS treated steel substrates was organized as a Nyquist plot and is shown in Figure 15. The charge transfer resistance was calculated from this plot by averaging five highest  $Z_{\text{real}}$  (x-axis) values for each sample. Real impedance values were used because the curve started to loop and averaging the five highest points gave relative charge transfer resistances at consistent frequency points.

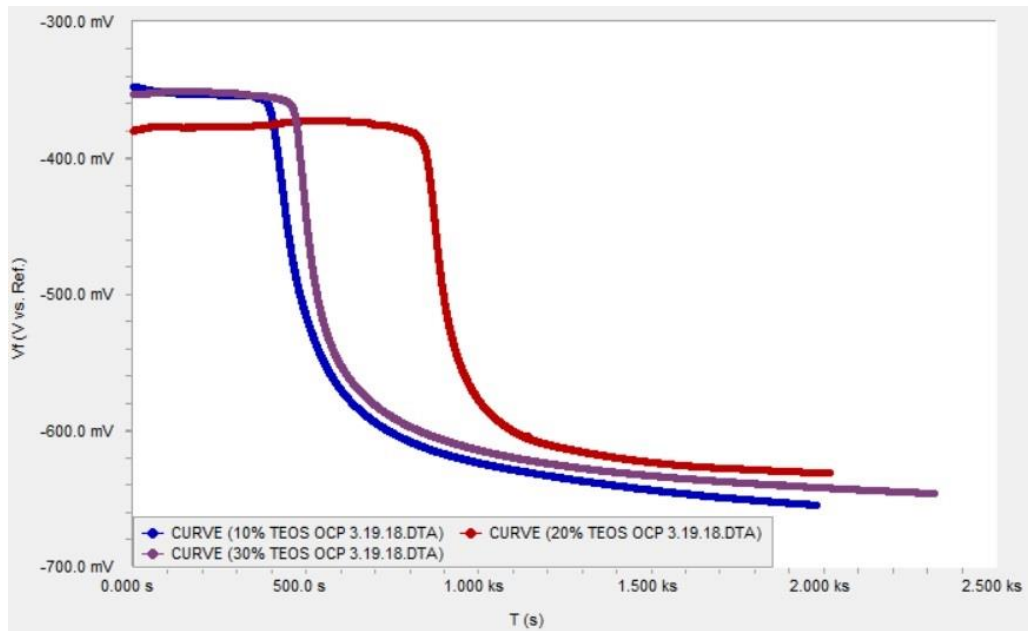


**Figure 14:** Open Circuit Potential of EIS/EFM Samples

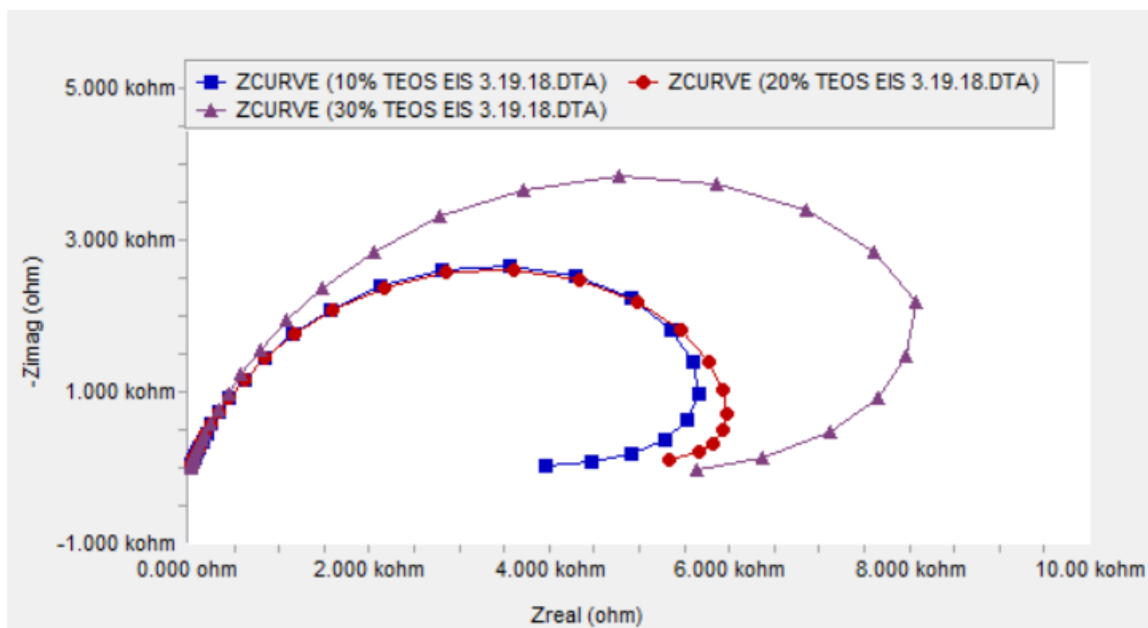


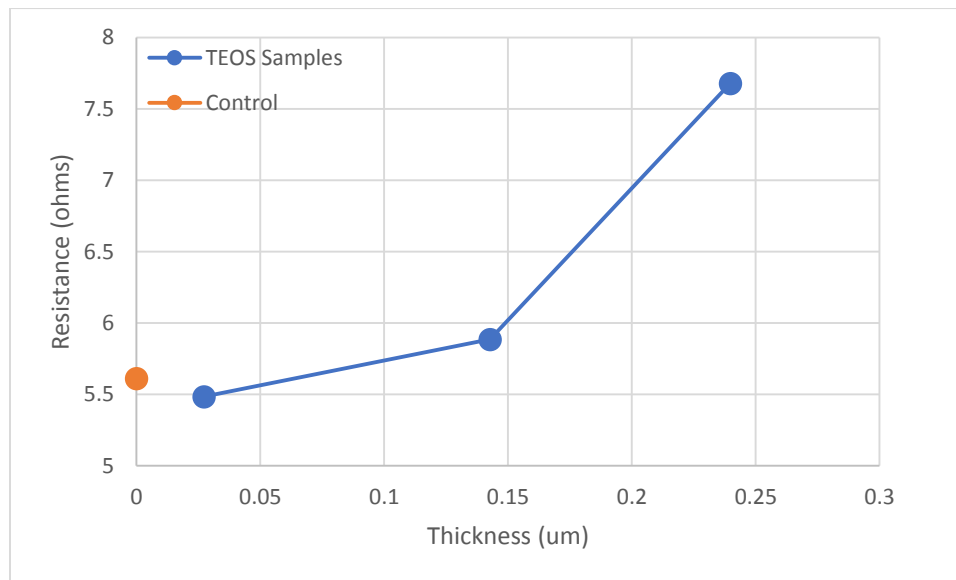
**Figure 15:** Nyquist plot of TEOS Samples

**Table 5:** EIS and EFM Results.

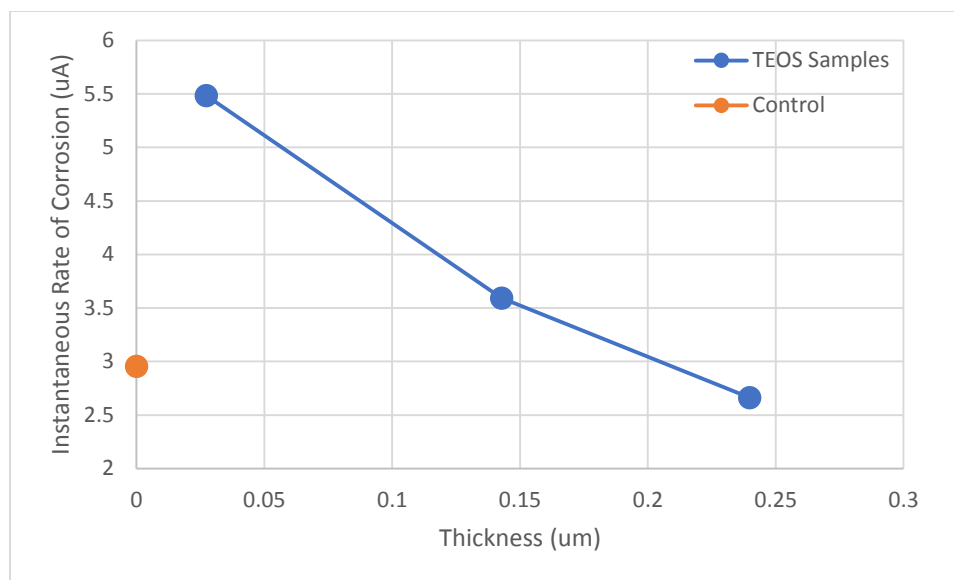
Sample	Charge Transfer Resistance (ohms)	Instantaneous Rate of Corrosion (microamps)
Control	5.614	2.956
10% TEOS	5.486	5.486
20% TEOS	5.885	3.592
30% TEOS	7.681	2.662

Table 5 reports the charge transfer resistances and instantaneous rates of corrosion for each of the samples. The charge transfer resistance was shown to increase as the TEOS thickness increased. In turn, the instantaneous corrosion rate decreased as the TEOS thickness increased. Both trends are illustrated in Figures 16 and 17, respectively. These results were unsurprising because, as the concentration of the silane network on the substrate increases, the resistance to the electrochemical reaction should also increase

while also decreasing the rate of the corrosion reactions. Because there were quantitative differences in the EIS and EFM data that were not linear, it shows that the increasing TEOS percentage is not solely increasing the size of the silane network in the Z direction. The higher TEOS percentage must also be changing the bulk network connectivity. If a higher percentage only increased the thickness of the network, then the differences in charge transfer resistance and instantaneous corrosion values would likely be linear in that doubling the thickness doubles the charge transfer resistance or halves the instantaneous rate of corrosion. Since they were not linear and water exclusion is improving as TEOS percentage increases, it can be concluded that increasing the TEOS content changes the network connectivity as well as the thickness.



**Figure 16:** Charge Transfer Resistance vs. Silane Thickness.



**Figure 17:** Instantaneous Rate of Corrosion vs. Silane Thickness.

The untreated substrate had a higher resistance than the 10% TEOS sample, as well as a lower instantaneous rate of corrosion than the 10% and 20% TEOS sample. It was quite possible that the 10% and 20% TEOS samples were forming void areas at spaces that were untreated while encouraging water entrapment at the interface while the 30% TEOS and control samples did not. Also, slight unintentional differences in water content and pH may have been detrimental to the silane layer formation for the 10% and 20% samples as the pH can easily affect the metal interface, causing the control to perform better. These rationales could be the cause of the lower resistance and higher rates of corrosion than the control. Despite the control group performing better than some of the TEOS treated samples, the trends established in the TEOS samples still gave information about how important the silane density and structure on the substrate is to performance.

## Chapter V. Conclusions and Future Works

The properties that silane pretreatment networks exhibit are heavily dependent on the relative concentration and molar ratios of unreacted and reacted materials in solution. It was determined via IR Spectroscopy that by keeping the reactivity ratio of silane to water 1:1 in 30% silane solution, the most siloxane bonds were formed in the resulting network. This gave a more uniform and denser film relative to the other molar ratios investigated. This was validated by the fact that the 1:1 silane to water ratio had the greatest adhesion in the DAS samples that were tested. It was also found that by increasing the concentration of the TEOS solution, the charge transfer resistance increases non-linearly while the instantaneous rate of corrosion also decreases nonlinearly. By theoretically calculating the thickness of the silane pretreatment, a normalized curve was made to illustrate how charge transfer resistance and instantaneous rate of corrosion changes with increasing thickness and network structure, which was supported by consistent results.

While much was gained from this series of experiments, much more can still be done. For future works, experiments should be conducted to determine the best conditions to achieve the absolute minimal self-condensation in silane solutions. The APS experiment only proved that the 1:1, while self-condensing the least in solution, gave the most siloxane bonds in solid form. It could be further hypothesized that even lower water content or extremely high-water concentration could minimize self-condensation in solution and yield different properties.

Furthermore, from the data it was realized that a charge transfer resistance calibration curve needs to be established for TEOS pretreatments. While this experiment

performed gave vital information about the standard trend in resistance and silane thickness, a curve must be established to further provide useful information about the extent that TEOS pretreatments can affect charge transfer resistance. From there, a model may be able to be developed to gain an overall perspective about how charge transfer resistance can be manipulated for improvement or investigated to determine when a coating could fail.

## References

- <sup>1</sup>Sørensen, P. A., Kiil, S., Dam-Johansen, K., & Weinell, C. E. (2009). Anticorrosive coatings: A review. *Journal of Coatings Technology Research*.  
<https://doi.org/10.1007/s11998-008-9144-2>
- <sup>2</sup>Wicks, Z. W., & Wiley InterScience (Online service). (n.d.). *Organic Coatings: Science and Technology*.
- <sup>3</sup>Leng, A., Streckel, H., & Stratmann, M. (1998). The delamination of polymeric coatings from steel. Part 1: Calibration of the Kelvinprobe and basic delamination mechanism. *Corrosion Science*, *41*(3), 547–578.
- <sup>4</sup>Posner, R., Wapner, K., Stratmann, M., & Grundmeier, G. (2009). Transport processes of hydrated ions at polymer/oxide/metal interfaces. *Electrochimica Acta*, *54*(3), 891–899.
- <sup>5</sup>Greenfield, D., & Scantlebury, J. D. (2000). Blistering and Delamination Processes on Coated Steel. Retrieved February 13, 2017
- <sup>6</sup>Carreira, A. F., Pereira, A. M., Vaz, E. P., Cabral, A. M., Ghidini, T., Pigliaru, L., & Rohr, T. (2017). Alternative corrosion protection pretreatments for aluminum alloys. *Journal of Coatings Technology and Research*, *14*(4), 879–892.  
<https://doi.org/10.1007/s11998-017-9922-9>
- <sup>7</sup>Wang, P., & Schaefer, D. W. (2008). Why does Silane Enhance the Protective Properties of Epoxy Films? *Langmuir*, *24*(23), 13496–13501.  
<https://doi.org/10.1021/la8028066>
- <sup>8</sup>Bertho, J., Stolojan, V., Abel, M.-L., & Watts, J. F. (n.d.). The effect of silane incorporation on a metal adhesive interface: A study by electron energy loss spectroscopy.
- <sup>9</sup>Wang, J.-P.; Song, Y.; Wang, J.-K.; Zhou, Q.; Li, Z.; Han, Y.; Yang, S.; Li, G. L.; Qi, T. pH-Responsive Polymer Coatings for Reporting Early Stages of Metal Corrosion. *Macromol. Mater. Eng.* 2017, *302* (9), 1700128.
- <sup>10</sup>Zhai, Q.; Zhou, C.; Zhao, S.; Peng, C.; Han, Y. Kinetic Study of Alkoxysilane Hydrolysis under Acidic Conditions by Fourier Transform near Infrared Spectroscopy Combined with Partial Least-Squares Model. *Ind. Eng. Chem. Res.* 2014.
- <sup>11</sup>Rammelt, U., & Reinhard, G. (1992). Application of electrochemical impedance spectroscopy (EIS) for characterizing the corrosion-protective performance of organic coatings on metals. *Progress in Organic Coatings*, *21*(2–3), 205–226.

- <sup>12</sup>Deflorian, F., & Rossi, S. (2006). An EIS study of ion diffusion through organic coatings. *Electrochimica Acta*, 51(8–9), 1736–1744.  
<https://doi.org/10.1016/j.electacta.2005.02.145>
- <sup>13</sup>Deyab, M. A.; Essehli, R.; El Bali, B.; Lachkar, M. Fabrication and Evaluation of  $\text{Rb}_2\text{Co}(\text{H}_2\text{P}_2\text{O}_7)_2 \cdot 2\text{H}_2\text{O}$ /waterborne Polyurethane Nanocomposite Coating for Corrosion Protection Aspects. *RSC Adv.* 2017, 7 (87), 55074–55080.
- <sup>14</sup>Morikawa, A.; Iyoku, Y.; Kakimoto, M.; Imai, Y. Preparation of a New Class of Polyimide-Silica Hybrid Films by Sol-Gel Process. *Polym. J.* 1992, 24 (1), 107–113.